

# Linear Space-Time Diversity Receivers for the Downlink of UMTS with WCDMA

ANDREAS JAROSCH, DIRK DAHLHAUS

Communication Technology Laboratory, Swiss Federal Institute of Technology (ETH), Zurich, Switzerland  
{jarosch,dahlhaus}@nari.ee.ethz.ch

**Abstract.** Simple linear demodulation schemes exploiting the space and time diversity of the mobile radio channel are derived for the downlink of the Universal Mobile Telecommunication System (UMTS) employing wideband code-division multiple access (WCDMA). Using different stochastic models of the signals at the  $M \geq 1$  receiver antennas and different objective functions including minimum-mean square error (MMSE) and maximum-likelihood approaches, we obtain time-invariant and time-variant detection schemes which make use of channel and receiver parameter estimates being calculated upon observation of a single slot. It turns out that the bit-error rate (BER) of the conventional receiver carrying out a maximum-ratio combining w.r.t. time and space can be improved considerably, where the achievable gain depends critically on the accuracy of the aforementioned estimates. Efficient ways for implementation are proposed and quantified in terms of the computational complexity. Analytical approximations and simulations of the BER for different system parameters reveal that the schemes represent means to get robust against both channel fading and multiple access interference caused by multipath propagation.

## 1 INTRODUCTION

Data detection in the downlink of the Universal Mobile Telecommunication System (UMTS) Terrestrial Radio Access (UTRA) differs from the counterpart in the uplink in several aspects. Most important is the decentralized operation and the correspondingly lower receiver complexity as compared to the base station. For the latter, multiuser approaches have been proposed to mitigate the effect of interference which is the main factor limiting performance of a conventional detector (CD) in spectrally efficient mobile radio systems employing code-division multiple access (CDMA). In the downlink, multipath propagation destroys the orthogonality of the signals synchronously transmitted from a certain base station. In view of the unknown interference structure, strategies being in general different from the uplink have to be pursued to improve the performance of the CD. One way meeting the aforementioned requirement of a moderate receiver complexity is the use of linear detection schemes where the overall receiver including channel estimation is usually highly non-linear.

Cyclically shifted filter bank-type equalizers for interference suppression in wideband CDMA (WCDMA) systems with reasonable complexity usually require cyclostationary interference over sufficiently short cycles [1]. Due to the long codes used in WCDMA systems, however, symbol rate cyclostationarity is not satisfied and the cor-

responding receiver algorithms cannot be applied. In [2], linear schemes including zero forcing and best linear unbiased estimation as well as linear minimum mean-square error (LMMSE) detection have been investigated. While the first two schemes are limited in performance due to noise enhancement, the latter requires the inversion of a usually large matrix where an algorithm is provided for the calculation of the inverse. If the observation length is reduced to carry out single-symbol detection, the channel model employed does not completely take into account the interference caused by the channel dispersion which leads to an inaccurate model especially for high-rate codes and channels with large dispersion. As another consequence of the adopted signal model, the covariance matrix of the received signal is not Toeplitz so that efficient signal processing algorithms known for this case [3] cannot be applied. The precombining and postcombining interference suppression receivers proposed in [4] are not applicable in the case of long scrambling codes due to convergence problems. In [5], zero-forcing and LMMSE receivers are considered. However, for the latter, no proposal has been made how to estimate the correlation matrix of the received signal. Furthermore, the analysis is based exclusively on the output signal-to-interference-plus-noise-ratio (SINR) which cannot be related directly to the resulting bit-error rates (BER). An adaptive channel equalization based on an LMMSE approach is presented in [6] where it is claimed that the com-

plexity of the matrix inversion might be unacceptable in fast changing environments.

In this paper, we consider three linear detection schemes in the context of the UTRA WCDMA downlink. Apart from the use of interference suppression, increasing the number of receiver antennas provides additional spatial diversity which in turn improves performance w.r.t. both interference and channel fading. In the following, we assume a receiver equipped with  $M \geq 1$  sensors where the channel within one slot is time-invariant. Furthermore, the intercell interference is considered negligible as compared to the intracell interference. The slot synchronization is finalized and no a priori information about the interfering user signals is available for demodulation. In order to keep the receiver complexity low, we do not consider sophisticated channel estimation schemes [7], equalization on the basis of large observation intervals [2] or blind interference cancellation approaches [8, 9] which result in high implementation effort in the case of several sensors. Instead, the focus is on simple channel estimators, e.g. with decision feedback in conventional receivers, and time-invariant and time-variant equalizers over sufficiently short observation intervals for symbol detection. We consider two candidates and compare them to the CD. The first is a time-invariant equalizer derived from the one in [10] for uplink transmission. It is derived as a LMMSE scheme for restoring the transmitted chip sequence followed by the usual correlation receiver. The second one is based on a totally different approach. Unlike the CD where the noise superimposed on the signal of interest at the output of the dispersive channel is assumed to be an additive white Gaussian noise (AWGN) process, the scheme models the interference at the transmitter to be AWGN. A subsequent maximum-likelihood (ML) detection rule provides a time-variant equalizer which can also be interpreted as a whitening filter. To keep the complexity low, we consider the detection of a single symbol instead of a sequence estimation. For  $M = 1$ , an approximation of the resulting scheme can exploit the fact that the covariance matrix in the model is Toeplitz and, consequently, efficient algorithms [3] for the required matrix inversion can be applied.

In Section 2, the system is described in detail where we assume the original proposal of the UTRA WCDMA specifications as of June 1998 [11]<sup>1</sup>. In Section 3, we present the applied linear detection schemes for a given channel impulse response (CIR) and interference parameters. In Section 4, the estimation of all parameters needed for symbol detection is discussed. After the treatment of implementation issues in Section 5 the performance of the schemes for different system scenarios is investigated in Section 6 where, in particular, an approximation of the BER performance of the CD in the high signal-to-noise (SNR) regime for known CIRs is derived. Conclusions are drawn in Section 7.

<sup>1</sup>Since the actual specifications [12, 13] have preserved all the major features of [11], this is a minor issue.

Note that bold face symbols denote random variables or vector/matrix processes and the corresponding symbols in normal font denote the respective realizations, where the dimensions of the used quantities are defined in the text.

## 2 DOWNLINK SIGNAL MODEL

We consider dedicated physical channels (DPCH) consisting of dedicated physical control/data channels (DPCCH/DPDCH) in the downlink of UMTS with WCDMA. The random access and the frame synchronization are assumed finalized. For comparison purposes of the different demodulation schemes, we consider uncoded transmission. Upon insertion of reference symbols, transmit power-control (TPC) and transport-format indicator (TFI) bits from higher protocol layers into the payload of consecutive slots, the signal transmitted by a certain base station is segmented as shown in Figure 1. One slot consists

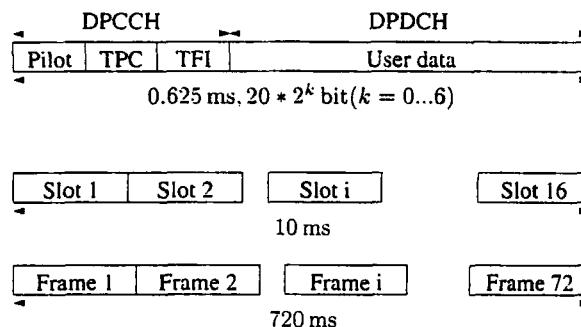


Figure 1: Frame format of a DPCH.

of 2560 chips. Upon mapping two consecutive information bits  $D_{k\Re}^{(i)} \in \{\pm 1\}$  and  $D_{k\Im}^{(i)} \in \{\pm 1\}$  to a quadrature shift-keying (QPSK) symbol  $D_k^{(i)} = D_{k\Re}^{(i)} + jD_{k\Im}^{(i)}$ , the complex baseband signal transmitted for the  $i$ -th symbol of the  $k$ -th user is given by

$$V_k^{(i)}(t) = G_k D_k^{(i)} C_k^{(i)}(t),$$

where  $G_k$  denotes the user specific gain. The spreading sequence

$$C_k^{(i)}(t) = \sum_{\nu=0}^{N_{ck}-1} C_{k;\nu}^{(i)} u(t - \nu T_c - i N_{ck} T_c)$$

with the chip duration  $T_c$  consists of a series of shifted chip pulses  $u(t)$  weighted by the chip  $C_{k;\nu}^{(i)}$  at regular intervals. The bit rate varies between 1280 and 20 bits per slot corresponding to a number of chips per symbol  $N_{ck} = 2^\nu$  with  $\nu = 2, \dots, 8$ . Due to the long scrambling codes involved in UTRA the spreading codes are different for all symbols within a frame. The base station (BS) transmits the sum of all signals of the  $K$  users in the considered cell from one

transmitter antenna via  $M$  time-variant multipath channels. The received signal at the  $m$ -th sensor can be expressed as

$$Y_m(t) = \int_{-\infty}^{\infty} \sum_{k=1}^K \sum_i V_k^{(i)}(t-\tau) H_m(t, \tau) d\tau + N_m(t),$$

where the channel impulse response (CIR) modelled as

$$H_m(t, \tau) = \sum_{\ell=1}^{L_m} H_{\ell m}(t) \delta(\tau - \tau_{\ell m})$$

consists of  $L_m$  relevant paths with  $H_{\ell m}(t)$ ,  $\tau_{\ell m} \in \mathbb{R}$  and  $\delta(\cdot)$  denoting the complex amplitudes, the delays and the Dirac delta function, respectively. Furthermore, we assume  $0 \leq \tau_{\ell m} \leq N_D T_c$  where  $N_D$  characterizes the channel dispersion. The components of the vector  $N_m(t)$  modelling both intercell interference and thermal receiver noise represent independent complex zero-mean AWGN processes with

$$\mathbf{E} \{N_m(t) N_{m'}^*(u)\} = \sigma_N^2 \delta(t-u) \delta[m-m'],$$

where  $\mathbf{E}\{\cdot\}$ ,  $(\cdot)^*$  and  $\delta[\cdot]$  denote the expectation operator, complex conjugation and the Kronecker delta function, respectively. In the following, we base the demodulation of the received signal on the observation of one slot and assume the CIR to be time-invariant during the observation, i.e.  $H_{\ell m}(t) \approx H_{\ell m}$  for  $t \in [t_0, t_0 + 2560T_c)$ . After sampling the output of a chip matched filter at time instants  $t = pT_c$  and assuming  $\tau_{\ell m} = \theta_{\ell m} T_c$  with  $p, \theta_{\ell m} \in \mathbb{N}$  we obtain a discrete time representation of the signal model

$$Y_m[p] = \sum_k \sum_i W_{mk}^{(i)}[p] + N_m[p], \quad (1)$$

$$W_{mk}^{(i)}[p] = \sum_q \alpha_m[q] V_k^{(i)}[p-q], \quad (2)$$

$$\alpha_m[p] = \sum_{\ell=1}^{L_m} \alpha_{\ell m} \delta[p - \theta_{\ell m}], \quad (3)$$

$$V_k^{(i)}[p] = g_k D_k^{(i)} C_k^{(i)}[p], \quad (4)$$

$$C_k^{(i)}[p] = \sum_{\nu=0}^{N_{ck}-1} C_{k;\nu}^{(i)} \delta[p - \nu - iN_{ck}] \quad (5)$$

with  $\alpha_{\ell m} = G_{k_d} H_{\ell m}$ ,  $\theta_{\ell m} \in \{0, \dots, N_D\}$  and  $g_k = G_k/G_{k_d}$ , where  $k_d$  denotes the index of the desired user signal. In view of the spectral root raised cosine chip pulses in UTRA, we obtain Gaussian noise processes with  $\mathbf{E}\{N_m[p] N_{m'}^*[q]\} = \sigma_N^2 \delta[m-m'] \delta[p-q]$  as in the time-continuous case. Note that  $C_k^{(i)}[p]$  is zero for  $p < iN_{ck}$  and  $p \geq (i+1)N_{ck}$ . In [9], it has been shown that for  $\tau_{\ell m} \neq \theta_{\ell m} T_c$  the worst case loss of signal energy due to the sampling process is about 11%. In order to get a more suitable notation segments of the introduced discrete-time signals are composed into vectors. The spreading code shifted in time by  $\theta$  is denoted as

$$C_k^{(i;\eta,\lambda)}(\theta) = [C_k^{(i)}[\eta - \theta], \dots, C_k^{(i)}[\eta - \theta + \lambda - 1]]^T.$$

For zero-time shift  $\theta = 0$ , the vectors  $W_{mk}^{(i;\eta,\lambda)}$ ,  $N_m^{(\eta,\lambda)}$  and  $Y_m^{(\eta,\lambda)}$  are defined accordingly. Using the vector notation we can write the undisturbed received signal vector of the  $k$ -th user at the  $i$ -th sensor as

$$W_{mk}^{(i;\eta,\lambda)} = g_k D_k^{(i)} \sum_{\ell=1}^{L_m} \alpha_{\ell m} C_k^{(i;\eta,\lambda)}(\theta_{\ell m}). \quad (6)$$

By stacking the signal vectors of all sensors, we define

$$W_k^{(i;\eta,\lambda)} = [W_{1k}^{(i;\eta,\lambda)T}, \dots, W_{Mk}^{(i;\eta,\lambda)T}]^T \quad (7)$$

and accordingly  $N^{(\eta,\lambda)}$  and  $Y^{(\eta,\lambda)}$ .

In order to write the convolution of the transmitted signal and the CIR as a matrix-vector product we define the channel matrix

$$A_m^{(\lambda)} = \begin{bmatrix} \alpha_m[N_D] \cdots \alpha_m[0] & 0 & \cdots & 0 \\ 0 & \ddots & \ddots & \vdots \\ \vdots & \ddots & \ddots & 0 \\ 0 & \cdots & 0 & \alpha_m[N_D] \cdots \alpha_m[0] \end{bmatrix} \quad (8)$$

with  $A_m^{(\lambda)} \in \mathbb{C}^{\lambda \times (\lambda + N_D)}$  and  $[A_m]_{pq} = \alpha_m[p - q + N_D]$ . Upon stacking the channel matrices according to

$$A^{(\lambda)} = [A_1^{(\lambda)T}, \dots, A_M^{(\lambda)T}]^T, \quad (9)$$

we can write the information signal at the receiver as

$$W_k^{(i;\eta,\lambda)} = g_k D_k^{(i)} A^{(\lambda)} \bar{C}_k^{(i;\eta,\lambda)} \quad (10)$$

with  $\bar{C}_k^{(i;\eta,\lambda)} = C_k^{(i;\eta,\lambda + N_D)}(N_D)$ . Note that  $\dim(\bar{C}_k^{(i;\eta,\lambda)}) = \dim(W_{mk}^{(i;\eta,\lambda)}) + N_D$ . Finally the total received signal is given by

$$Y^{(\eta,\lambda)} = \sum_i \sum_k g_k D_k^{(i)} A^{(\lambda)} \bar{C}_k^{(i;\eta,\lambda)} + N^{(\eta,\lambda)}. \quad (11)$$

### 3 DETECTION SCHEMES

In this section, different linear detectors are derived where estimates  $\hat{A}^{(\lambda)}$  of  $A^{(\lambda)}$  and all other receiver parameters are assumed given. The parameter estimation is discussed in Section 4.

#### 3.1 CONVENTIONAL DETECTOR

For reference purposes, we formulate the CD in terms of the aforementioned signal vectors. It is well known [14]

that in the CD, the overall noise process including intersymbol interference (ISI), intercell interference (ICI), multiple access interference (MAI) and thermal noise is modelled as an AWGN process. Consequently, for this model, given values  $\bar{C}_k^{(i;\eta,\lambda)} = \bar{C}_k^{(i;\eta,\lambda)}$ , an estimate  $A^{(\lambda)} = \hat{A}^{(\lambda)}$  and a hypothesis  $D_k^{(i)} = D_{k_d}^{(i)}$  in (10), the CD carries out a matched filtering of the observation containing all samples depending on  $D_k^{(i)}$ . Thus, we choose  $\eta = iN_{c k_d}$  and  $\lambda = N_{c k_d} + N_D$  where we suppress the both indices for better readability subsequently whenever their value is obvious from the context. Using the corresponding observation  $Y$ , we obtain upon employing the ML rule

$$\begin{aligned} \hat{D}_{k_d}^{(i)} &= \arg \max_{D_{k_d}^{(i)}} \Re \left\{ \left( W_{k_d}^{(i)} \right)^H Y \right\} \\ &= \arg \max_{D_{k_d}^{(i)}} \Re \left\{ \left( D_{k_d}^{(i)} \right)^* Z_{k_d}^{(i)} \right\} \end{aligned} \quad (12)$$

with the decision variable

$$Z_{k_d}^{(i)} = \left( \bar{C}_{k_d}^{(i)} \right)^T \hat{A}^H Y \quad (13)$$

to be calculated by summing the output signals of rake receivers at the different sensors. Obviously the maximisation in (12) can be done separately for the real and imaginary part of  $D_{k_d}^{(i)}$ . This leads to the bit estimates

$$\hat{D}_{k_d \Re}^{(i)} = \text{sgn} \left( \Re \left\{ Z_{k_d}^{(i)} \right\} \right) \quad (14)$$

$$\hat{D}_{k_d \Im}^{(i)} = \text{sgn} \left( \Im \left\{ Z_{k_d}^{(i)} \right\} \right). \quad (15)$$

The receiver structure with the CD is depicted in Figure 2.

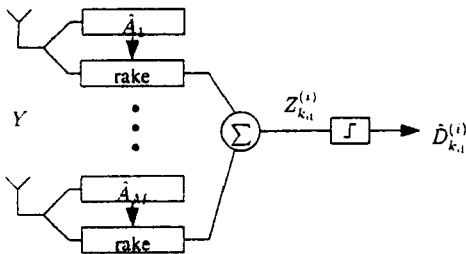


Figure 2: Receiver structure with CD.

### 3.2 LINEAR TIME-INVARIANT EQUALIZATION

In this section, we modify the linear time-invariant equalizer proposed in [10] for the uplink of a WCDMA system and apply it for downlink demodulation. The structure of the equalizer derived subsequently using an MMSE criterion is shown in Figure 3. As can be concluded from the figure, the equalization is done on chip level and followed by a subsequent correlation with the segment of the

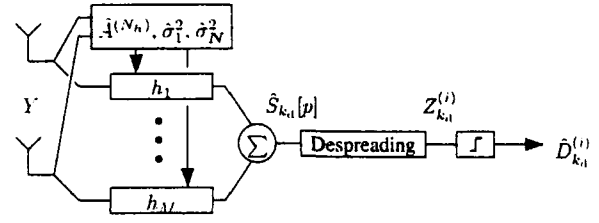


Figure 3: Receiver structure with LMMSE detector.

spreading sequence. Upon defining

$$S_k[p] = \sum_{i'} D_k^{(i')} C_k^{(i')}[p] \quad (16)$$

as the weighted transmitted chip sequence and the vector

$$S_k^{(\eta,\lambda)} = [S_k[\eta], \dots, S_k[\eta + \lambda - 1]]^T$$

the received signal in (11) can be written as

$$Y^{(\eta,\lambda)} = \sum_k g_k \hat{A}^{(\lambda)} S_k^{(\eta-N_D, \lambda+N_D)} + N^{(\eta,\lambda)}. \quad (17)$$

The equalizer is defined by the filter taps

$$\begin{aligned} h_m &= [h_{m1}, \dots, h_{mN_h}]^T \in \mathbb{C}^{N_h \times 1} \\ h &= [h_1^T, \dots, h_{M_I}^T]^T \in \mathbb{C}^{N_h M_I \times 1} \end{aligned}$$

where  $N_h$  taps are applied at each sensor to equalize the linear signal distortions caused by the transmission channel. The output signals of the filters<sup>2</sup> combined over the sensors

$$\hat{S}_{k_d}[p] = h^H Y^{(p, N_h)} \quad (18)$$

provide an estimate of the chip sequence (16). Despreading leads to the decision variable

$$Z_{k_d}^{(i)} = \sum_{\nu=0}^{N_{c k_d}-1} \hat{S}_{k_d}[iN_{c k_d} + \nu] C_{k_d}^{(i)\nu}. \quad (19)$$

To determine the filter coefficients the mean-square error

$$\begin{aligned} J &= \mathbf{E} \left\{ \left| \hat{S}_{k_d}[p] - S_{k_d}[p] \right|^2 \right\} \\ &= h^H \mathbf{R}_Y h - h^H \mathbf{R}_{Y S} - \mathbf{R}_{S Y} h + 2 \end{aligned} \quad (20)$$

with the autocorrelation matrix

$$\mathbf{R}_Y = \mathbf{E} \left\{ Y^{(p, N_h)} \left( Y^{(p, N_h)} \right)^H \right\} \quad (21)$$

and the cross correlation vector

$$\mathbf{R}_{Y S} = \mathbf{E} \left\{ Y^{(p, N_h)} S_{k_d}[p]^* \right\} \quad (22)$$

<sup>2</sup>Note that these filters are noncausal but the notation is simple. The corresponding causal filters would have the form  $\hat{S}_{k_d}[p] = h^H Y^{(p-N_h+1, N_h)}$ .

is minimized. This leads to the well known discrete-time Wiener filter solution

$$h = \mathbf{R}_Y^{-1} \mathbf{R}_{YS}. \quad (23)$$

Inserting (17) into (21) and exploiting the assumption of i.i.d. bit and chip sequences we obtain

$$\mathbf{R}_Y = \sigma_1^2 \hat{A}^{(N_h)} \left( \hat{A}^{(N_h)} \right)^H + \sigma_N^2 \mathbf{I}_{N_h M} \quad (24)$$

with

$$\sigma_1^2 = 2 \sum_k g_k^2. \quad (25)$$

The corresponding procedure leads to

$$\mathbf{R}_{YS} = 2 \hat{A}^{(N_h)} e_{N_D+1} \quad (26)$$

with  $e_q = [0, \dots, 0, 1, 0, \dots, 0]^T$ . For given  $\hat{A}^{(N_h)}$ ,  $\sigma_1^2$  and

$\sigma_N^2$ , the Wiener filter coefficients (23) are determined by (24) and (26). Note that  $\mathbf{R}_Y$  and  $\mathbf{R}_{YS}$  do not depend on  $p$ , i.e. they are time independent and the whole receiver is time-invariant. Estimators for the aforementioned parameters will be derived in Section 4. For later use we insert (18) into (19) and obtain

$$Z_{k_d}^{(i)} = \sum_{\nu=0}^{N_{ck_d}-1} 2C_{k;\nu}^{(i)} e_{N_D+1}^T \times \left( \hat{A}^{(N_h)} \right)^H \mathbf{R}_Y^{-1} Y^{(iN_{ck_d}+\nu, N_h)}. \quad (27)$$

### 3.3 LINEAR TIME-VARIANT EQUALIZATION

#### 3.3.1 Interference model

The equalizer derived in the previous section is based on the minimization of the expected error in (20) using the assumption of i.i.d. chip and bit sequences. In this section, we will take a slightly different route starting from a statistical model of the transmitted signal and apply a ML detection rule to the received signal. In order to derive the model, we assume a sufficiently large number of simultaneously transmitted i.i.d. signals and apply the central limit theorem (CLT) [15]. As a consequence, unlike the conventional detector assuming the information signal of interest embedded in AWGN at the receiver, we model the interference at the transmitter to represent an AWGN process while we keep the assumption of Gaussian thermal noise at the receiver according to (1). The overall disturbance is thus an additive colored Gaussian noise process with a spectrum depending clearly on the CIR which has to be estimated at the receiver for carrying out a coherent detection.

With  $\eta = iN_{ck_d}$  and  $\lambda = N_{ck_d} + N_D$ , the received signal vector  $\mathbf{Y}^{(\eta, \lambda)}$  contains all samples depending on the

symbol  $D_{k_d}^{(i)}$ . Due to the Gaussian model, we can immediately identify the ML rule for detection of  $D_{k_d}^{(i)}$ . Suppressing the dependence of the signal on  $\eta$  and  $\lambda$  for simplicity, the signal model in (11) can be rewritten as

$$\mathbf{Y} = D_{k_d}^{(i)} \hat{A} \bar{C}_{k_d}^{(i)} + \hat{A} \bar{Q} + N \quad (28)$$

with

$$\bar{Q} = \sum_{i'} \sum_{k'} g_{k'} D_{k'}^{(i')} \bar{C}_{k'}^{(i')} \quad (29)$$

$(i', k') \neq (i, k_d)$

containing all ISI and MAI terms. As outlined above,  $\bar{Q}$  is modelled as AWGN resulting in a colored Gaussian process  $\hat{A} \bar{Q}$ .

#### 3.3.2 Detection scheme for given parameters

According to [16] the joint probability density function of  $\mathbf{Y}$  is given as

$$p_Y(\mathbf{Y} | D_{k_d}^{(i)}, \hat{A}) = \frac{1}{\pi^{M\lambda} |\mathbf{C}_Y|} \times \exp \left\{ -(\mathbf{Y} - \mathbf{E}\{\mathbf{Y}\})^H \mathbf{C}_Y^{-1} (\mathbf{Y} - \mathbf{E}\{\mathbf{Y}\}) \right\} \quad (30)$$

with the covariance matrix  $\mathbf{C}_Y$  of the received signal to be defined below. The ML detection rule for  $D_{k_d}^{(i)}$  is

$$\hat{D}_{k_d}^{(i)} = \arg \max_{D_{k_d}^{(i)}} p_Y(\mathbf{Y} | D_{k_d}^{(i)}, \hat{A}) \quad (31)$$

$$= \arg \max_{D_{k_d}^{(i)}} \Re \left\{ \left( D_{k_d}^{(i)} \right)^* \left( \bar{C}_{k_d}^{(i)} \right)^T \hat{A}^H \mathbf{C}_Y^{-1} \mathbf{Y} \right\}. \quad (32)$$

Thus, we obtain the detection rules (14) and (15) where, however, the decision variable in (13) is replaced by

$$Z_{k_d}^{(i)} = \left( \bar{C}_{k_d}^{(i)} \right)^T \hat{A}^H \mathbf{C}_Y^{-1} \mathbf{Y}. \quad (33)$$

Thus, the received signal is first multiplied by the matrix  $\hat{A}^H \mathbf{C}_Y^{-1}$  and subsequently correlated with the code  $\bar{C}_{k_d}^{(i)}$ .

To detect the symbol according to (32) we have to calculate  $\mathbf{C}_Y = \mathbf{E} \left\{ (\mathbf{Y} - \mathbf{E}\{\mathbf{Y}\}) (\mathbf{Y} - \mathbf{E}\{\mathbf{Y}\})^H \right\}$ . Using (28) and (29), we obtain

$$\mathbf{C}_Y = \mathbf{E} \left\{ \hat{A} \bar{Q} \bar{Q}^H \hat{A}^H \right\} + \mathbf{E} \{ N N^H \} = \hat{A} \mathbf{C}_{\bar{Q}} \hat{A}^H + \sigma_N^2 \mathbf{I}_{M(N_{ck_d} + N_D)} \quad (34)$$

with  $\mathbf{C}_{\bar{Q}} = \mathbf{E} \left\{ \bar{Q} \bar{Q}^H \right\}$ . Inserting (29), exploiting the orthogonality of the different user signals at the transmitter and assuming mutually independent symbols and chips each modelled as i.i.d. random variables we get

$$\mathbf{C}_{\bar{Q}} = \text{diag} \left( \underbrace{\sigma_1^2, \dots, \sigma_1^2}_{N_D}, \underbrace{\sigma_0^2, \dots, \sigma_0^2}_{N_{ck_d}}, \underbrace{\sigma_1^2, \dots, \sigma_1^2}_{N_D} \right) \quad (35)$$

with  $\sigma_1^2$  in (25) and  $\sigma_0^2 = \sigma_1^2 - 2$ . Note that the lower triangular matrix  $F$  received by the Cholesky decomposition  $C_Y = FF^H$  is known as whitening filter [17]. Furthermore,  $C_Y$  is a diagonal matrix for non-dispersive channels and  $Z_{k_d}^{(i)}$  in (33) becomes a scaled version of  $Z_{k_d}^{(i)}$  in (13). As a consequence, in view of the orthogonality of the OVSF codes, the detector in (32) exhibits the same optimality as the CD for this special case. If the number of users in the considered cell is large we can simplify the scheme by the approximation  $\sigma_0^2 \approx \sigma_1^2$  so that (34) simplifies to

$$C_Y = \sigma_1^2 \hat{A} \hat{A}^H + \sigma_N^2 I_{M(N_{ck_d} + N_D)}. \quad (36)$$

Simulations show that this approximation has almost no influence on the BER even for scenarios with a small number of user signals. The resulting scheme is termed colored noise detector (CND). Since in general  $\hat{A}^H C_Y^{-1}$  is not a Toeplitz matrix, the CND cannot be implemented as a time-invariant linear filter, but constitutes a linear time-variant one [17]. Note that the filter is time-variant w.r.t. the chip index within one symbol, but time-invariant for consecutive symbols, given that the channel remains constant. Thus the time-variance of the filter is due to the channel dispersion, not due to the scrambling code sequence and the filter has to be recalculated only upon a change of the CIR. The receiver structure with the CND is depicted in Figure 4.

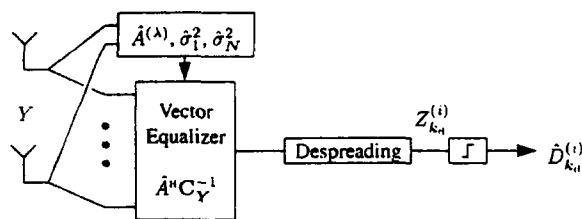


Figure 4: Receiver structure with CND.

### 3.3.3 Comparison of the MMSE based receiver and the CND

Although the decision variables in (27) and (33) look similar to each other, there are substantial differences in both equalization schemes. In (18), the restored signal at the output of the equalizer at time  $p$  depends only on the samples  $Y[p] \dots Y[p + N_h - 1]$  while all samples in the restored signal in (33) depend in general on  $Y[iN_{ck_d}] \dots Y[(i+1)N_{ck_d} + N_D - 1]$ . While the former scheme can be implemented as a continuously running filter, the latter operates on successive blocks of data. Concerning the covariance matrices in (24) and (36) involved in the equalization, we observe identical structures with, however, different matrix dimensions according to the aforementioned different observation lengths of  $Y$ . Finally, for a given value  $N_D$ , in the LMMSE scheme the filter length  $N_h$  has to be chosen heuristically while the equalizer length

of  $(N_{ck_d} + N_D)$  in the CND arises from the ML scheme employed.

## 4 PARAMETER ESTIMATION

In this section, we present several procedures for estimating the parameters used in the different detectors presented in the previous section. As before, our goal is to devise schemes of moderate complexity which can be combined with the linear detectors. Upon channel estimation in Section 4.1, we consider a simple scheme for estimating  $\sigma_1^2$  and  $\sigma_N^2$  in Section 4.2.

### 4.1 CHANNEL ESTIMATION

In contrast to the CD both equalizers of Section 3 inherently take into account the MAI caused by other intracell users. In both schemes, the performance of the interference suppression depends critically on the accuracy of the estimated channel matrix  $\hat{A}$ . It is calculated in the conventional receiver in a simple correlation type estimator using the pilot symbols in the DPCCH transmitted in each slot<sup>3</sup>. In spite of the interference limitation of the CD, its BER performance using the obtained channel estimates the decision variable (13) usually allows for decision feedback of the detected symbols in order to increase the observation window to the whole slot and consequently to increase the accuracy of the channel estimates. The corresponding procedure is described below where we assume a maximum observation length of one slot. A further improvement not being considered here is to increase the observation window which possibly necessitates a channel model with an increased number of parameters.

We consider a set  $D_p = \{D_{k_d}^{(i)} | i \in \mathcal{M}\}$  of known pilot bits in the DPCCH forming a preamble to the information symbols of the slot, where  $\mathcal{M}$  denotes a suitable index set. Furthermore, the slot synchronization is assumed given and the spreading code sequence  $C = \{\bar{C}_{k_d}^{(i;\eta,\lambda)}\}$  for all  $i$  of the whole slot is known at the receiver. If we model the MAI in the CD as AWGN, we can write the received signal as

$$Y^{(\eta,\lambda)} = \sum_{i \in \mathcal{M}} W_{k_d}^{(i;\eta,\lambda)} + Q^{(\eta,\lambda)} + N^{(\eta,\lambda)},$$

where  $Q^{(\eta,\lambda)}$  and  $N^{(\eta,\lambda)}$  denote spatially and temporally white Gaussian processes with  $Q^{(\eta,\lambda)} = \sum_{k' \neq k_d} \sum_i W_{k'}^{(i;\eta,\lambda)}$  and  $E \left\{ Q^{(\eta,\lambda)} \left( Q^{(\eta,\lambda)} \right)^H \right\} = \sigma_Q^2 I_{M\lambda}$

The values  $\eta = j_s N_{cps}$  and  $\lambda = N_p N_{ck_d} + N_D$  are chosen to include all samples in the received signal depending on the pilot symbols where  $N_p$  is the number of symbols

<sup>3</sup>In the current release of UTRA, there is a common pilot channel which can be used in the same way as the estimator outlined here to improve the estimation accuracy.

in  $D_p$ . Upon defining the vector of all channel parameters  $\Theta = \{\Theta_1, \dots, \Theta_M\}$  with  $\Theta_m = \{\Theta_{1m}, \dots, \Theta_{Lm}\}$  and  $\Theta_{\ell m} = \{\alpha_{\ell m}, \theta_{\ell m}\}$ , the ML estimate is defined by

$$\hat{\Theta} = \arg \max_{\Theta} \Lambda(\Theta) \quad (37)$$

with the log-likelihood function (LLF)

$$\Lambda(\Theta) = \sum_{m=1}^M \left( \Re \left\{ \sum_{i \in \mathcal{M}} \left( W_{mk_d}^{(i)} \right)^H Y_m \right\} - \frac{1}{2} \left\| \sum_{i \in \mathcal{M}} W_{mk_d}^{(i)} \right\|^2 \right). \quad (38)$$

A simplification of (38) results for sufficiently large values  $\lambda$  if we neglect the cross-correlation between different paths in the second sum in view of the long scrambling codes. Upon substitution of  $W_{mk_d}^{(i)}$  from (6), the second term simplifies to

$$\frac{1}{2} \left\| \sum_{i \in \mathcal{M}} W_{mk_d}^{(i)} \right\|^2 = N_p N_{ck_d} \sum_{\ell=1}^{L_m} |\alpha_{\ell m}|^2$$

and the LLF can be written as

$$\Lambda(\Theta) = \sum_{m=1}^M \sum_{\ell=1}^{L_m} \Lambda_m(\alpha_{\ell m}, \theta_{\ell m}) \quad (39)$$

with  $\theta_{\ell m} \neq \theta_{\ell' m}$  for  $\ell \neq \ell'$  and

$$\Lambda_m(\alpha, \theta) = \Re \left\{ \alpha^* \sum_{i \in \mathcal{M}} \left( D_{k_d}^{(i)} C_{k_d}^{(i)}(\theta) \right)^H Y_m \right\} - N_p N_{ck_d} |\alpha|^2. \quad (40)$$

The maximization of the whole function can be accomplished by maximizing  $\Lambda_m(\alpha, \theta)$  separately for each path at each sensor. Finally, upon maximizing  $\Lambda_m(\alpha, \theta)$  w.r.t.  $\alpha$  and inserting the solution into (40), we obtain

$$\hat{\theta}_{\ell m} = \arg \max_{\theta} \left| \sum_{i \in \mathcal{M}} \left( D_{k_d}^{(i)} C_{k_d}^{(i)}(\theta) \right)^H Y_m \right|^2 \quad (41)$$

$$\hat{\alpha}_{\ell m} = \frac{1}{2N_p N_{ck_d}} \sum_{i \in \mathcal{M}} \left( D_{k_d}^{(i)} C_{k_d}^{(i)}(\hat{\theta}_{\ell m}) \right)^H Y_m. \quad (42)$$

These estimates can be used to detect all information symbols of the slot according to (14) and (15). The aforementioned feedback is carried out by increasing  $\lambda = N_p N_{ck_d} + N_D$  to  $\lambda = N_{\text{sym}, k_d} N_{ck_d} + N_D$ , where  $N_{\text{sym}, k_d}$  denotes the number of symbols per slot for user  $k_d$ , and repeating the estimation for each path using both pilot and detected information symbols. For typical BER values of the CD using the estimates in (41) and (42) with  $\lambda = N_p N_{ck_d} + N_D$  the feedback procedure almost always leads to improved estimates. This is due to the fact that the degradation caused by few erroneously detected information symbols is usually much less than the improvement obtained by averaging the interference over a considerably larger observation interval.

## 4.2 ESTIMATION OF $\sigma_1^2$ AND $\sigma_N^2$

For the estimation of  $\sigma_1^2$  and  $\sigma_N^2$  we consider (36). If we assume that the model in (28) holds, the matrix  $C_Y$  is given and the channel parameters are estimated perfectly, i.e.  $\hat{A} = A$ , any two linearly independent equations defining the elements of  $C_Y$  in (36) can be used to calculate  $\sigma_1^2$  and  $\sigma_N^2$ . In the following, we extend this algebraic scheme for determining  $\sigma_1^2$  and  $\sigma_N^2$  to the case where the above assumptions are violated.

To this end, we write the defining equations for one diagonal and one off-diagonal element of  $C_Y$  explicitly according to

$$\begin{aligned} [C_Y]_{pp} &= \sigma_1^2 [\hat{A}\hat{A}^H]_{pp} + \sigma_N^2 \\ [C_Y]_{pq} &= \sigma_1^2 [\hat{A}\hat{A}^H]_{pq}, \end{aligned}$$

which is a system of two linear equations in the two unknown parameters with  $p, q \in [1, \dots, M\lambda]$ . The relation between the row and column indices  $p$  and  $q$  and the sensor indices  $m$  and  $m'$  is defined as  $m = (p-1)\text{div}\lambda$  and  $m' = (q-1)\text{div}\lambda$ , where  $x \text{ div } y$  denotes the division of  $x$  by  $y$  rounded towards zero. The time shift corresponding to the difference of the matrix indices  $p$  and  $q$  is calculated as  $\theta = ((q-1)\text{mod}\lambda) - ((p-1)\text{mod}\lambda)$  which gives  $\theta = q-p$  in the single sensor case, i.e. for  $m = m'$ , where  $x \text{ mod } y$  denotes the remainder upon division of  $x$  by  $y$ . We define

$$\begin{aligned} b_{pq} &= [\hat{A}\hat{A}^H]_{pq} \\ &= \sum_r \hat{\alpha}_m [p-r+N_D] \alpha_{\ell m}^* [q-r+N_D] \\ &= \sum_s \hat{\alpha}_m [s] \alpha_{\ell m}^* [s+\theta] \end{aligned} \quad (43)$$

with  $s = p-r+N_D$ . The elements  $[C_Y]_{pq}$  are estimated by sample averages where an additional simplification arises from replacing the *covariance* by the *correlation* matrix in order to circumvent the subtraction of the desired user signal from  $Y$  prior to averaging. This simplification is reasonable for a sufficiently large number of interferers. The corresponding sample estimates are given by

$$\hat{c}_{pq} = [\hat{C}_Y]_{pq} = \frac{1}{\lambda'} \left( Y_m^{(\eta', \lambda')} \right)^T \left( Y_{m'}^{(\eta'+\theta, \lambda')} \right)^*. \quad (44)$$

From the resulting system

$$\begin{aligned} \hat{c}_{pp} &= \sigma_1^2 b_{pp} + \sigma_N^2 \\ \hat{c}_{pq} &= \sigma_1^2 b_{pq} \end{aligned}$$

we obtain the solution

$$\hat{\sigma}_1^2 = \frac{\hat{c}_{pq}}{b_{pq}} \quad (45)$$

$$\hat{\sigma}_N^2 = \hat{c}_{pp} - \frac{\hat{c}_{pq} b_{pq}}{b_{pq}} \quad (46)$$

In view of the generally complex valued expressions  $\hat{c}_{pq}$  and  $b_{pq}$ , we force  $\hat{\sigma}_1^2$  and  $\hat{\sigma}_N^2$  to take real non-negative values by modifying (45) and (46) according to

$$\hat{\sigma}_1^2 = \left| \frac{\hat{c}_{pq}}{b_{pq}} \right| \quad (47)$$

$$\hat{\sigma}_N^2 = \left| \hat{c}_{pp} - \frac{\hat{c}_{pq} b_{pp}}{b_{pq}} \right|. \quad (48)$$

Finally, the indices  $p$  and  $q$  are chosen according to the coefficients  $b_{pp}$  and  $b_{pq}$  having the largest absolute values. In order to find these largest values we evaluate (43) for all  $m, m'$  and  $\theta$ . The objective here is to minimize the impact of random errors on the estimates  $b_{pp}$  and  $b_{pq}$ . As discussed in Section 6, the estimation of  $\sigma_1^2$  and  $\sigma_N^2$  need not be very accurate and the approximations made above are usually not critical.

## 5 IMPLEMENTATION ISSUES

All detectors in Section 3 use the channel estimates obtained from the feedback procedure in Section 4.1. The complexity of the channel estimation can be derived immediately from (41) and (42) and is not considered here. Furthermore, we neglect the slight complexity increase in the time-variant equalizer due to the operations required for estimating  $\sigma_1^2$  and  $\sigma_N^2$  in Section 4.2. The main complexity differences of the receivers arise from the use of the different detectors and thus we will investigate the number of arithmetic operations in one slot. In receivers with  $M > 1$  like e.g. cars or trains, computational complexity is often not as critical as in receivers with  $M = 1$  like e.g. a hand set. Thus, we consider an efficient procedure for the matrix inversions in (27) and (33) for  $M = 1$  in Section 5.1. In Section 5.2, the complexity is characterized for  $M > 1$  and a simplification is proposed to reduce the computational effort for matrix inversion in the case of multiple sensors. In Section 5.3 the total complexity of the detectors including the matched filter and interference mitigation parts is discussed.

The following complexity considerations are based on the algorithms (13), (27), and (33). The complexity of the algorithms is expressed as the number of arithmetic operations. In this context an operation is defined as one complex multiplication and one complex addition. Complex divisions and subtractions are treated as multiplications and additions, respectively.

### 5.1 SINGLE SENSOR

The complexity of the inversion of a general invertible matrix is in the order of  $n^3$  operations, i.e.  $O(n^3)$ , where  $n$  denotes the dimension of the matrix [18]. In the single sensor case, i.e.  $M = 1$ , the matrices  $\mathbf{R}_Y$  and  $\mathbf{C}_Y$  according

to (24) and (36) are Toeplitz and Hermitian. For the inversion of such a well structured matrix, Trench has proposed an efficient algorithm of complexity  $O(n^2)$  [19, 3] which we adopt for implementing the required filter operations<sup>4</sup>.

### 5.2 MULTIPLE SENSORS

For  $M > 1$ , the matrices  $\mathbf{R}_Y$  and  $\mathbf{C}_Y$  are still Hermitian, but not Toeplitz anymore. To the best of our knowledge there exists no efficient algorithm for the inversion of that kind of matrices resulting in a complexity of  $O(n^2)$ . Since the dimensions of  $\mathbf{C}_Y$  grow with the length of the scrambling code, the size of  $\mathbf{C}_Y$  is very large for lower data rates and some kind of approximation has to be considered. According to (36) the matrix  $\mathbf{C}_Y$  consists of block matrices

$$\mathbf{C}_{Y_{m,m'}} = \sigma_1^2 \hat{A}_m \hat{A}_{m'}^H + \delta [m - m'] \sigma_N^2 \mathbf{I}_{N_{ck_d} + N_D}.$$

Neglecting cross-covariance terms between different sensors, i.e. setting  $\mathbf{C}_{Y_{m,m'}} = 0$  for  $m \neq m'$  the inverse of  $\mathbf{C}_Y$  is the block diagonal matrix

$$\mathbf{C}_Y^{-1} = \text{diag} \left( \mathbf{C}_{Y_{1,1}}^{-1}, \dots, \mathbf{C}_{Y_{M,M}}^{-1} \right) \quad (49)$$

and the block matrices  $\mathbf{C}_{Y_{m,m'}}^{-1}$  can be efficiently calculated using the Trench algorithm mentioned in Section 5.1. The detector neglecting cross-covariance terms at different sensors is called simplified CND (SCND).

### 5.3 DETECTOR COMPLEXITY

In addition to the matrix inversion which is needed once per slot, matched filtering and interference mitigation have to be executed once per symbol. The matched filter part, i.e. the term  $(\tilde{\mathbf{C}}_{k_d}^{(i)})^T \hat{A}^n$  in (13) and (33) is the same for the CD, CND and the SCND. From the comparison of (36) and (49), it follows that the number of operations for interference mitigation, i.e. the calculation of  $\mathbf{C}_Y^{-1} Y$  in the CND is  $M$  times higher than in the SCND. The matched filtering and interference mitigation in (27) cannot be separated for the LMMSE. The complexity of the different terms in the calculation of the different decision variables is summarized in Table 1.

## 6 PERFORMANCE EVALUATION

In this section, the performance of the different receivers is characterized in terms of the average BER. The latter is investigated as a function of the average signal-to-noise ratio (SNR) for several system scenarios differing in

<sup>4</sup>A further complexity reduction can be achieved by exploiting the fact that for  $M = 1$  a Toeplitz band matrix has to be inverted [20].

Table 1: Detector complexity (approximate number of complex multiplications and additions) of the CD, LMMSE, CND and SCND.

Purpose		matched filter	interference mitigation
Operation	matrix inversion	vector-matrix-vector product	matrix-vector product
Once per	slot	symbol	
CD	-	$N_{ck_d}(M(N_{ck_d} + N_D) + 1)$	-
$M = 1$			
LMMSE	$N_h^2$	$N_{ck_d}N_h(N_h + 1)$	
CND	$(N_{ck_d} + N_D)^2$	same as CD	$(N_{ck_d} + N_D)^2$
$M > 1$			
LMMSE	$(MN_h)^3$	$N_{ck_d}MN_h(MN_h + 1)$	
CND	$M^3(N_{ck_d} + N_D)^3$	same as CD	$M^2(N_{ck_d} + N_D)^2$
SCND	$M(N_{ck_d} + N_D)^2$	same as CD	$M(N_{ck_d} + N_D)^2$

the number of users, i.e. the system load, the length of the signature codes, the number of receiver antennas as well as the accuracy of the channel impulse response estimates. Upon definition of the average SNR we characterize the detection performance of the conventional receiver for high SNR values using a Gaussian approximation in order to estimate the performance without the need for extensive simulations. A realistic performance characterization has to take into account the imperfect channel estimation. The latter is investigated in simulations presented for different situations w.r.t. the aforementioned parameters. Special attention is given to the required accuracy of parameters in the colored noise detector and the sensitivity of the BER against errors of the channel parameter estimates.

### 6.1 BER APPROXIMATION FOR THE CD

The BER of the  $k$ -th receiver is characterized as a function of the average SNR defined by

$$\bar{\gamma} = \mathbf{E} \left\{ \frac{E_b^{(i)}}{\sigma_N^2} \right\} = \frac{\bar{E}_b}{\sigma_N^2},$$

where the expectation is w.r.t. the scrambling codes and the channel fading according to  $E_b^{(i)} = g_k^2 (\bar{C}_k^{(i)})^T A^H A \bar{C}_k^{(i)}$ . Analytical expressions for the BER are hard to find since the decision variables of the receivers depend on the received signal in a highly non-linear way due to channel estimation and decision feedback. However, if we restrict the analysis to the CD and assume perfect channel estimates, simple approximations of the BER can be found. To this end, we consider the decision variable of the CD conditioned on all parameters but the channel noise

$$Z_{\mathcal{R}} = \Re \left\{ g_k (\bar{C}_k^{(i)})^T A^H Y | A, \bar{C}, D \right\}.$$

Since  $Z_{\mathcal{R}}$  is conditionally Gaussian, the conditional bit-error probability (BEP) reads [14]

$$P_b = \frac{1}{4} (\text{erfc}(\zeta^+) + \text{erfc}(\zeta^-)), \quad (50)$$

where  $\zeta^{\pm} = \mu^{\pm} / (\sqrt{2}\sigma^{\pm})$ ,  $\text{erfc}(\cdot)$  is the complementary error function and  $\mu^{\pm}$  and  $\sigma^{\pm}$  denote the mean and variance, resp., of the decision variable for  $D_k^{(i)} = \pm 1$ . In view of the scrambling codes and the mutually independent data streams of different users [9], we model the aforementioned parameters as conditionally Gaussian random variables according to

$$\mu^{\pm} = \pm \bar{E}_b + \Gamma, \quad \sigma^{\pm 2} = \frac{1}{2} \sigma_N^2 (\bar{E}_b + 2\Upsilon) \quad (51)$$

with<sup>5</sup>

$$\Gamma | A \sim \mathcal{N}(0; \sigma_{\Gamma}^2), \quad \Upsilon | A \sim \mathcal{N}(0; \sigma_{\Upsilon}^2) \quad (52)$$

and

$$\sigma_{\Gamma}^2 = N_{ck_d} \left( \sum_{k'} g_{k'}^2 \right) \sum_{m=1}^M \sum_{m'=1}^M \sum_{\ell=1}^{L_m} \sum_{\ell' \neq \ell}^{L_{m'}} \delta[\theta_{\ell m} - \theta_{\ell m'}] \delta[\theta_{\ell' m} - \theta_{\ell' m'}] \times \Re \{ \alpha_{\ell m}^* \alpha_{\ell' m} \alpha_{\ell m'} \alpha_{\ell' m'}^* \}. \quad (53)$$

While  $\Upsilon$  depends on the autocorrelation function of  $\bar{C}_k^{(i)}$  [9],  $\Gamma$  contains weighted crosscorrelation values between  $\bar{C}_k^{(i)}$  and  $\bar{C}_{k'}^{(i')}$ . This leads to the assumption of conditional independence of the joint density function [9]

$$p_{\Gamma, \Upsilon | A}(\Gamma, \Upsilon | A) = p_{\Gamma | A}(\Gamma | A) p_{\Upsilon | A}(\Upsilon | A)$$

<sup>5</sup>The fact that  $\sigma^{\pm 2}$  in (51) can be negative is irrelevant for the subsequent derivation.

and thus

$$p_{\Gamma, \Upsilon, A}(\Gamma, \Upsilon, A) = p_{\Gamma|A}(\Gamma|A)p_{\Upsilon|A}(\Upsilon|A)p_A(A). \quad (54)$$

The average BEP is given by  $\bar{P}_b = \mathbb{E}\{P_b\}$ , where the expectation is w.r.t.  $\Gamma, \Upsilon$  and  $A$ . In view of (50),  $\bar{P}_b$  cannot be calculated analytically. However, for the limiting case  $\sigma_N^2 \rightarrow 0$ , we have

$$\text{ind}^\pm(\Gamma) = \text{erfc}(\zeta^\pm) \Big|_{\sigma_N^2 \rightarrow 0} = \begin{cases} 2 & \text{for } \mp\Gamma > \bar{E}_b \\ 0 & \text{for } \mp\Gamma \leq \bar{E}_b \end{cases} \quad (55)$$

and with (52) and (54)

$$\begin{aligned} \bar{P}_b &= \int \frac{1}{4} (\text{ind}^+(\Gamma) + \text{ind}^-(\Gamma)) p_{\Gamma, \Upsilon, A}(\Gamma, \Upsilon, A) d\Gamma d\Upsilon dA \\ &= \int \frac{1}{2} \text{erfc}\left(\frac{\bar{E}_b}{\sqrt{2}\sigma_\Gamma}\right) p_A(A) dA. \end{aligned} \quad (56)$$

This is the desired approximation for the BER of the CD in the high SNR domain. It can be evaluated in simulations by averaging the expression  $\frac{1}{2} \text{erfc}\left(\frac{\bar{E}_b}{\sqrt{2}\sigma_\Gamma}\right)$  over the different realizations of  $A$ .

### 6.2 SIMULATION RESULTS

The different schemes have been investigated in extensive Monte-Carlo simulations for different scenarios. The time-variant channel impulse responses (CIR) are created according to the stochastic radio channel model (SRCM) in [21] where four clusters of waves impinge at the receiver. In each cluster, there are 10 waves with identical delays and different incidence angles. The velocity of the mobile is 100 km/h and the channel excess delay is about 3  $\mu$ s. The CIR results from sampling the SRCM once per slot. Figure 5 shows the absolute value of the CIR at the first sensor for 100 consecutive slots. figure absCIR As can be seen, the

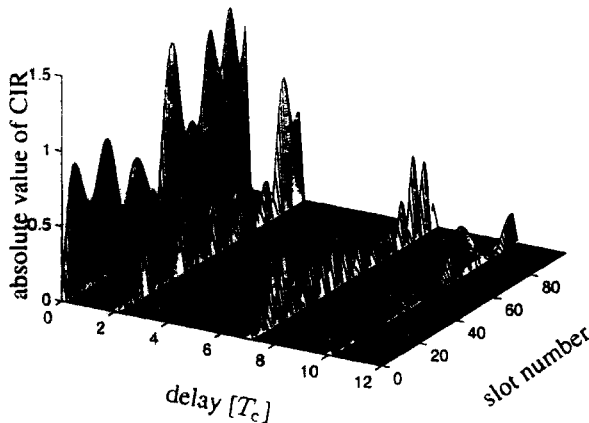


Figure 5: Absolute value of the channel impulse responses at one sensor used in the simulations.

superposition of the ten waves results in fading amplitudes for each cluster. The number of equalizer coefficients per sensor of the LMMSE is chosen to be  $N_h = 12$  for all simulations. For each point on each of the subsequent BER curves, a total of  $10^6$  transmitted bits have been simulated.

First, we consider a receiver with  $M = 1$  antenna and a scenario with  $N_{ckd} = 16$  and  $K = 8$ , which corresponds to a system load of 50 %. As mentioned above, the channel estimation is carried out during one slot where 10 % of the symbols are assumed to be pilot symbols. In the case of decision feedback, they are used to initialize the channel parameter estimates. The number of clusters is assumed given at the receiver. In Figure 6, the BER values are plotted for the different receivers. BER1 The dash-dotted

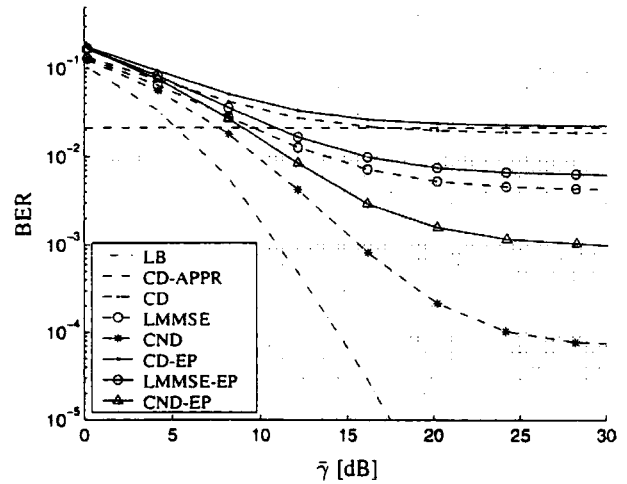


Figure 6: BER for  $M = 1, N_{ckd} = 16$  and  $K = 8$ .

curve results from averaging the BEP in AWGN over the channel statistics and thus represents a lower bound. The approximation of the CD for a given CIR is labelled as CD-APPR. To characterize the impact of the channel estimation on the achievable BER, we first consider the case of a known CIR at the receiver. As can be concluded from Figure 6, the CND shows the best detection performance where the BER saturates at  $\bar{P}_b \approx 8 \cdot 10^{-5}$ . There is an increasing gain of the CND as compared to the LMMSE detector for increasing SNR values, where the BER of the LMMSE saturates at  $\bar{P}_b \approx 1 \cdot 10^{-3}$ . The interference limitation of the CD leads to a saturation at  $\bar{P}_b \approx 2.5 \cdot 10^{-2}$  which is close to the value given by (56). The corresponding curves for estimated parameters (EP) are labelled as CND-EP, LMMSE-EP and CD-EP. As can be concluded from the figure, the performance loss of the CND-EP is about 2 dB for  $\bar{\gamma} < 12$  dB, while the saturation level is increased considerably. The losses of the LMMSE-EP and the CD-EP are about the same, where the saturation level increase is less emphasized than in the case of the CND. Interestingly, the CND-EP outperforms the LMMSE with

perfect channel knowledge while it is sensitive to channel estimation errors. If we increase the load to 100 %, i.e.  $K = 16$ , we obtain the BER in Figure 7.

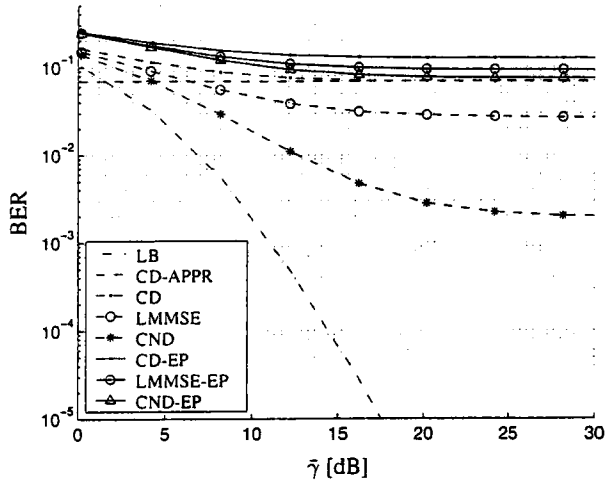


Figure 7: BER for  $M = 1$ ,  $N_{ck_d} = 16$  and  $K = 16$ .

While the performance differences are comparable to the case of  $K = 8$  for known channels, the performance is almost the same for the case where the channel has to be estimated. This clearly indicates that the BER performance depends critically on the accuracy of the channel estimates.

The interference in the CND is based on the assumption of an AWGN process at the transmitter. To validate the robustness against derivations from the model, we consider the case of a single interferer for the case of the minimum value  $N_{ck} = 4$  for  $k = 1, 2$  which corresponds again to a system with 50 % load. The resulting BER are shown in Figure 8. Although the central limit theorem is obviously

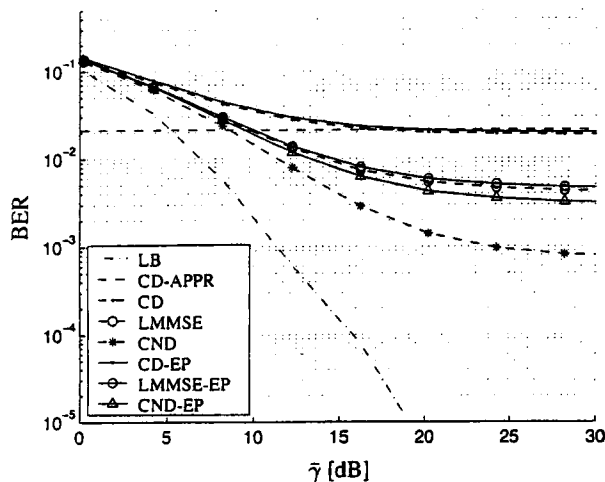


Figure 8: BER for  $M = 1$ ,  $N_{ck_d} = 4$  and  $K = 2$ .

not satisfied in this situation, the CND still outperforms the other detection schemes and achieves a lower BER for estimated channel parameters than the LMMSE for known channels. Again, an improved channel estimation leads to an improved BER of the CND, especially for high SNR values.

The spatial diversity of the mobile radio channel can be exploited to improve the BER performance. In Figure 9, we consider the scenario of Figure 6, however for the case of  $M = 3$  antennas. Obviously, all schemes can benefit from

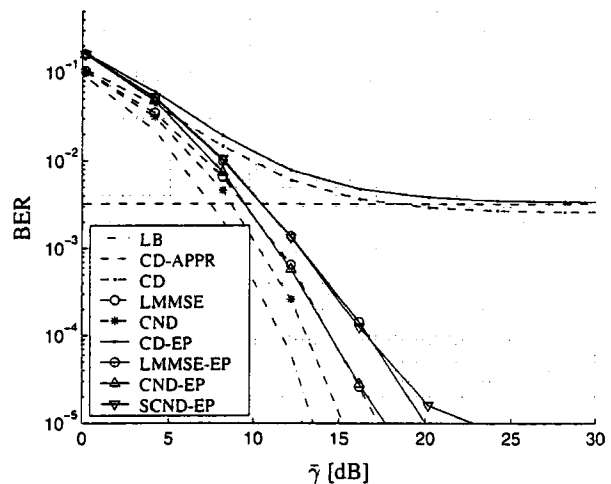


Figure 9: BER for  $M = 3$ ,  $N_{ck_d} = 16$  and  $K = 8$ .

the increased diversity. The equalizers do not show a BER saturation in the considered SNR range and the differences between the CND and the LMMSE are less emphasized. The BER of the SCND-EP and the LMMSE-EP is about the same for  $\bar{\gamma} \leq 16$  dB, while for  $\bar{\gamma} > 16$  dB the LMMSE-EP outperforms the SCND-EP. Note that the BER of the CND shows a loss of less than 2 dB as compared to the lower bound.

In Figure 10, we increase again the load to 100 %, i.e.  $K = 16$ . Surprisingly, the performance for given channels does not change very much for the LMMSE and the CND equalizers as compared to the case of  $K = 8$ . However, as soon as the channel estimation errors are taken into account, all equalizers perform equally well with a saturation level of about  $\bar{P}_b \approx 1.5 \cdot 10^{-2}$  which is a third of the corresponding value of the CD-EP. For completeness, we consider the case of a single interferer in Figure 11 with  $M = 3$  and  $N_{ck_d} = 4$ . The behaviour of the schemes is similar to the case of Figure 8. In particular, the CND is still superior to the LMMSE for both known and estimated channels. In this respect, the modelling of a discrete-valued interference process as AWGN does not lead to a performance degradation. Note that the BER of the CND-EP is substantially lower as compared to the SCND-EP at the expense of an increased complexity.

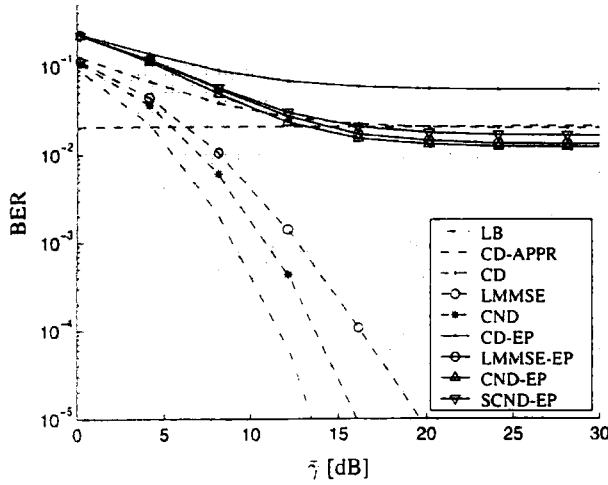


Figure 10: BER for  $M = 3$ ,  $N_{ck_d} = 16$  and  $K = 16$ .

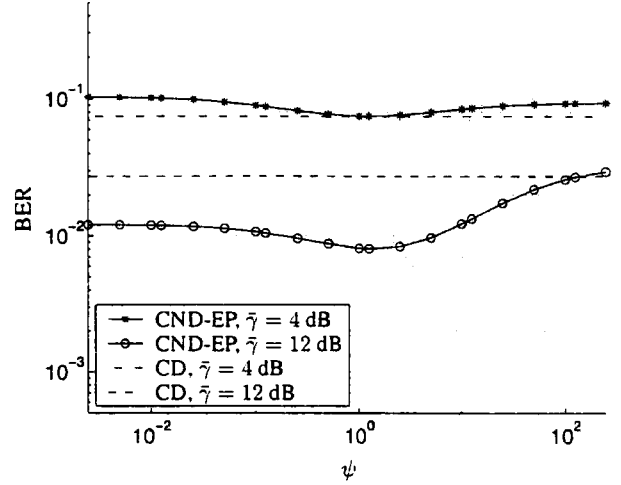


Figure 12: BER as a function of  $\psi$  for the the system in Figure 6.

### 7 CONCLUSIONS

In this paper, several linear demodulation schemes are derived for the UTRA FDD downlink and compared for different system parameters, e.g. the system load, the number of receiver antennas, and the spreading code length. In order to allow for a large maximum mobile speed, the procedure for estimating the parameters needed for symbol detection is based on the observation of only one slot. The simplest scheme is the conventional receiver carrying out a maximum-ratio combining w.r.t. time and space. After formulating a time-invariant equalizer based on a MMSE approach, we derive a time-variant equalizer resulting from a maximum-likelihood approach where the interference at the transmitter is modelled as an AWGN process. It turns out that the increased degrees of freedom in the time-variant equalizer can be exploited for decreasing the BER as compared to the time-invariant one, where the latter already outperforms the conventional receiver. The achievable gain depends critically on the accuracy of the parameter estimation procedure which is based on a decision feedback from the conventional receiver for complexity reasons. In a practical system, the parameter estimation can be improved by extending the observation interval or including the estimation of the Doppler frequency. It has been shown that even for the channel estimation considered here, the BER of the time-variant equalizer is rather insensitive to errors in the estimation of the relative noise contribution of multiple access interference and thermal noise. For highly accurate parameter estimates, three receiver antennas, and a system load of 50 %, the BER of the scheme is within 2 dB of a lower bound for the corresponding fading channel. The schemes can be implemented efficiently for the case of one receiver antenna using the Trench algorithm. In the multisensor case, the complexity of the equalizers can be reduced by neglecting the correlation between

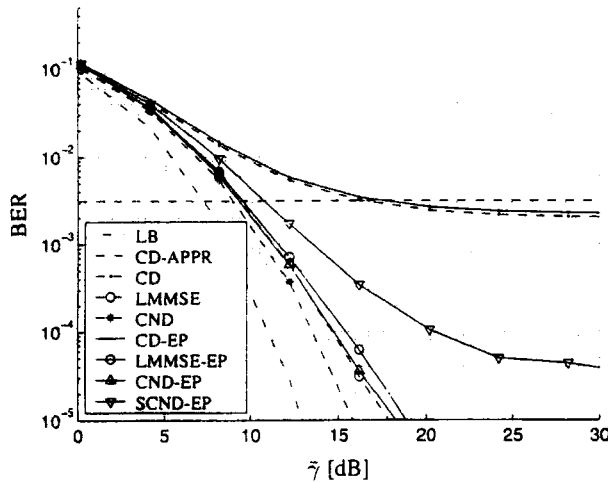


Figure 11: BER for  $M = 3$ ,  $N_{ck_d} = 4$  and  $K = 2$ .

An important parameter in the CND is the ratio  $\sigma_{rel}^2 = \sigma_N^2 / \sigma_I^2$  which controls the relative noise contribution in the decision variable caused by the interfering signals and the thermal noise. In Figure 12, we consider the dependence of the BER on  $\psi = \hat{\sigma}_{rel}^2 / \sigma_{rel}^2$  with  $\hat{\sigma}_{rel}^2 = \hat{\sigma}_N^2 / \hat{\sigma}_I^2$  for the system in Figure 6 where the parameters have been estimated. The minimum BER is obtained for  $\psi = 1$  which is the optimum point if the model assumptions hold. As can be concluded from a close inspection of Figure 6 and Figure 12, the channel estimates are sufficiently accurate in order not to move the minimum BER away from the above value due to random errors. Furthermore, the variations of the BER around  $\psi = 1$  are moderate which indicates that for given channel parameter estimates the estimation of  $\hat{\sigma}_{rel}^2$  does not have to be very accurate and, consequently, the CND-EP performance is robust against this source of error.

signals at different sensors at the expense of a BER degradation depending on the system parameters.

*Manuscript received on June 1, 2001.*

## REFERENCES

- [1] M. Latva-aho. Bit error probability analysis for FRAMES WCDMA downlink receivers. *IEEE Trans. Veh. Tech.*, 47(4):1119–1133, November 1998.
- [2] S. Werner and J. Lilleberg. Downlink channel decorrelation in CDMA systems with long codes. In *Proc. of the 49th IEEE Vehicular Technology Conference*, Vol. 2, pages 1614–17, Houston, Texas, 16–20 May 1999.
- [3] S. Zohar. Toeplitz Matrix Inversion: The Algorithm of W. F. Trench. *Journal of the Association for Computing Machinery*, 16(4):592–601, October 1969.
- [4] M. Latva-aho. *Advanced Receivers for Wideband CDMA Systems*. PhD thesis, Univ. Oulu, Finland, Acta Universitatis Ouluensis, 1998.
- [5] I. Ghauri and D. T. M. Slock. Linear receivers for the DS-CDMA downlink exploiting orthogonality of spreading sequences. *32nd Asilomar Conf. on Sig., Syst. and Comp.*, Vol. 1, pages 650–654, 1998.
- [6] M.J. Heikkilä, P. Komulainen, and J. Lilleberg. Interference suppression in CDMA downlink through adaptive channel equalization. In *Proc. of the 50th IEEE Vehicular Technology Conference (VTC '99-Fall)*, Vol. 2, pages 978–982, 1999.
- [7] A.J. Weiss and B. Friedlander. CDMA downlink channel estimation with aperiodic scrambling. In *Proc. of the 31st Asilomar Conf. on Signals, Systems & Computers*, Vol. 2, pages 828–832, Pacific Grove, CA, November 1997.
- [8] D. Dahlhaus, A. Jarosch, and Z. Cheng. Smart antenna concepts for the UMTS terrestrial radio access. In *Proc. of the Smart Antenna Workshop, European Microwave Week*, pages 73–92, Munich, Germany, October 1999.
- [9] A. Jarosch. *Verfahren zur robusten Demodulation in der Abwärtsstrecke von UMTS mit breitbandigem Codevielfachzugriff*, Vol. 9 of *Series in Broadband Communication*. Hartung-Gorre, Konstanz, Germany, 2001.
- [10] H. Liu and M.D. Zoltowski. Blind equalization in antenna array CDMA systems. *IEEE Trans. on Sig. Proc.*, 45(1):161–172, January 1997.
- [11] ETSI. The ETSI UMTS Terrestrial Radio Access (UTRA) ITU-R RTT Candidate Submission. <http://www.itu.org>. June 1998.
- [12] 3GPP, TSG-RAN. Physical channels and mapping of transport channels onto physical channels (FDD), (3G TS 25.211). <ftp://ftp.3gpp.org/Specs>, 1999 and later.
- [13] 3GPP, TSG-RAN. Spreading and modulation (FDD), (3G TS 25.213). <ftp://ftp.3gpp.org/Specs>, 1999 and later.
- [14] J.G. Proakis. *Digital Communications*. McGraw-Hill, New York, NY, 2nd edition, 1989.
- [15] A. Papoulis. *Probability, Random Variables, and Stochastic Processes*. McGraw-Hill, New York, NY, 2nd edition, 1991.
- [16] A. van den Bos. The multivariate complex normal distribution – a generalization. *IEEE Trans. Inform. Theory*, 41(2):537–539, March 1995.
- [17] H.V. Poor. *An Introduction to Signal Detection and Estimation*. Springer-Verlag, New York, NY, 2nd edition, 1994.
- [18] G. Strang. *Linear Algebra and its Application*. Harcourt Brace Jovanovich, Inc., 3rd edition, 1988.
- [19] W.F. Trench. An Algorithm for the Inversion of Finite Toeplitz Matrices. *Journal of the Society for Industrial and Applied Mathematics*, 12(3):515–522, September 1964.
- [20] W.F. Trench. Inversion of Toeplitz Band Matrices. *Mathematics of Computation*, 28(128):1089–1095, October 1974.
- [21] R. Heddergott, U. P. Bernhard, and B. H. Fleury. Stochastic radio channel model for advanced indoor mobile communication systems. In *Proc. of the 8th IEEE Int. Symp. on Personal, Indoor and Mobile Radio Communications (PIMRC '97)*, Vol. 1, pages 140–144, Helsinki, Finland, September 1997.